ELSEVIER

International Journal of Solids and Structures 41 (2004) 1605–1624

INTERNATIONAL JOURNAL OF SOLIDS and STRUCTURES

www.elsevier.com/locate/ijsolstr

# Transient analysis of viscoelastic helical rods subject to time-dependent loads

Beytullah Temel *

*Department of Civil Engineering, University of Çukurova, 01330 Balcalı-Adana, Turkey*

Received 16 January 2003; received in revised form 15 September 2003

**Abstract**

The transient analysis of viscoelastic helical rods subject to time-dependent loads are examined in the Laplace domain. The governing equations for naturally twisted and curved spatial rods obtained using the Timoshenko beam theory are rewritten for cylindrical helical rods. The curvature of the rod axis, effect of rotary inertia and, shear and axial deformations are considered in the formulation. The material of the rod is assumed to be homogeneous, isotropic and linear viscoelastic. The viscoelastic constitutive equations are written in the Boltzmann–Volterra form. Ordinary differential equations in canonical form obtained in the Laplace domain are solved numerically using the complementary functions method to calculate the dynamic stiffness matrix of the problem. The solutions obtained are transformed to the real space using an appropriate numerical inverse Laplace transform method. Numerical results for quasi-static and dynamic response of viscoelastic models are presented in the form of graphics.


*Keywords:* Boltzmann–Volterra theory; Viscoelastic materials; Helical spring; Inverse Laplace transforms

## 1. Introduction

The dynamic behaviour of helical bars and curved rods is an important engineering problem. In practice, helical bars are used as structural elements known as helical stairs and as mechanical elements in vehicle suspension systems and motor valve springs. To simplify the analysis, it is generally assumed that the material is elastic. However, in reality, the materials are vicoelastic due to internal friction, and thus the viscoelastic constitutive relations yield more realistic results than the elastic constitutive relations with regard to the material behaviour.

In many research papers, the dynamic response of viscoelastic materials are investigated using various models.

The application of the Laplace transform to viscoelastic beams was presented by Flügge (1975). Kıral et al. (1976) presented the equations of motion for viscoelastic curved rods, however, they did not solve the

* Tel.: +90-322-3386563; fax: +90-322-3386126.
*E-mail address:* btemel@cukurova.edu.tr (B. Temel).

0020-7683/$ - see front matter 
doi:10.1016/j.ijsolstr.2003.09.054

problem effectively. They used the transfer matrix method in their analysis. The method of maximum degree of precision was used for Laplace inversion which provided accurate results for one period only or for a short time.

Findley et al. (1976) used the correspondence principle and the superposition principle for solving the governing equations of the viscoelastic beam. Christensen (1982) reported the transient response of the viscoelastic beam using the Fourier transform. The above studies are based on the fact that the governing equations of viscoelasticity can be converted to the equations of elasticity by integral transformations. For complex geometries and constitutive relations, closed form solutions are often not possible and numerical solution techniques should be adopted.

The application of the finite element method to the complex geometry has been presented by a number of authors. White (1986) used the constitutive law of hereditary integral type, in which the time interval form is approximated by the finite difference method to perform a finite element analysis in a quasi-static problem. Adey and Brebbia (1973) used an approximate inversion procedure to obtain the inversion solution of the associated elastic problem. Chen and Lin (1982) studied the dynamic response of a beam using a creep law of time hardening to model the viscoelastic material. Yamada et al. (1974) reported the natural frequency of a viscoelastic beam and a rod.

Chen (1995) studied the linear viscoelastic Timoshenko beam for quasi-static and dynamic response. He assumed that the Poisson ratio is constant and only elasticity modulus is viscoelastic. The relaxation modulus is expressed by the same Prony series for both normal stress–strain and shear stress–strain relations. The hybrid method is used to remove the time parameter using the Laplace transform and the associated equation is solved using the finite element method.

Aköz and Kadıoğlu (1996) examined a mixed finite element for elastic circular beams using Gâteaux differential. Using a similar approach Aköz and Kadıoglu (1999) has studied the quasi-static and dynamic analysis of viscoelastic Timoshenko and Euler–Bernoulli beams. Kadıoğlu and Aköz (1999) studied the general forms of relaxation modulus for both Poisson ratio and Young modulus for quasi-static and dynamic response of circular beams. In order to remove the time derivatives from the governing equations and boundary conditions, the method of the Laplace–Carson transform was utilised.

Ilyasov and Aköz (2000) examined static and dynamic behaviour of plates. The viscoelastic constitutive equations were written in the Boltzmann–Volterra form.

Park and Schapery (1999) presented and tested a numerical method of interconversion between modulus and compliance functions when the given and predicted functions are based on a Prony series representation of transient functions. Schapery and Park (1999) proposed and verified a simple approximate interconversion method by examples. Park (2001) examined different approaches to the mathematical modeling of viscoelastic dampers and compared their theoretical basis and performance.

Kim and Kim (2001) studied the parametric instability of a laminated beam subjected to a periodic loading. The governing equations were derived from Hamilton's principle with Bolzmann's superposition principle for linear viscoelastic constitutive equations.

As mentioned above the viscoelastic models are commonly used in structures like straight beams, plates and shells. However, to the best of present authors' knowledge the viscoelastic analysis of helical bars have not been reported yet. In this research, the application of an efficient method to the viscoelastic analysis of helical bars will be presented.

Quasi-static and dynamic response of viscoelastic helical rods under time-dependent loads are investigated in the Laplace domain. The governing equations for naturally twisted and curved spatial rods obtained using the Timoshenko beam theory are rewritten for cylindrical helical rods. The curvature of the rod axis, effect of rotary inertia and, shear and axial deformations are considered in the formulation. The dynamic stiffness matrix of the problem is calculated in the Laplace transform space by applying the complementary functions method in Temel and Çalım (2003) to the differential equations in canonical form. The solutions obtained in the Laplace domain are then transformed to the time space using the

Durbin's inverse Laplace transform method (Durbin, 1974; Narayanan, 1979; Yerli et al., 1998). This provides great convenience in the solution of the problems having general boundary conditions. The desired accuracy is obtained by taking only a few elements as opposed to high number of elements (in the order of hundreds) needed in finite element analysis. Ordinary differential equations with variable coefficients can also be solved exactly in Laplace domain by using the complementary functions method. In the solution of viscoelastic helical rods, the Boltzmann–Volterra theory is considered. Numerical results for elastic–static, quasi-static, elastic–dynamic and viscoelastic dynamic responses of helical rods are presented.

## 2. Rod geometry

Consider a naturally curved and twisted spatial slender rod. The trajectory of geometric center $G$ of the rod is defined as the rod axis and its position vector at $t = 0$ is given by $\mathbf{r}^0 = \mathbf{r}^0(s, 0)$ where $s$ is measured from an arbitrary reference point $s = 0$ on the axis (Fig. 1a).

Let, at any time $t$, a moving reference frame be defined by unit vectors **t**, **n**, **b** with the origin of the axis of the rod is chosen such that

$$\mathbf{t} = \frac{\partial \mathbf{r}^0(s,t)}{\partial s} \tag{1}$$

where **t**, **n** and **b** are unit tangent, normal and binormal vectors respectively. The following differential relations among the unit vectors **t**, **n**, **b** can be obtained with the aid of the Frenet formulas (see Sokolnikoff and Redheffer, 1958)

$$\partial \mathbf{t}/\partial s = \chi \mathbf{n}, \quad \partial \mathbf{n}/\partial s = \tau \mathbf{b} - \chi \mathbf{t}, \quad \partial \mathbf{b}/\partial s = -\tau \mathbf{n} \tag{2}$$

where $\chi$ and $\tau$ are the curvature and the natural twist of the axis, respectively. It is noted that $\chi$ is always positive and that $\tau$ is positive for a clockwise rotation about **t** when advanced in the increasing $s$-direction. They are expressed in terms of the spatial derivatives of the position vector $\mathbf{r}^0(s,t)$:

$$\chi = \left| \frac{\partial^2 \mathbf{r}^0}{\partial s^2} \right|, \qquad \tau = -\frac{\frac{\partial \mathbf{r}^0}{\partial s} \cdot \frac{\partial^2 \mathbf{r}^0}{\partial s^2} \times \frac{\partial^3 \mathbf{r}^0}{\partial s^3}}{\chi^2} \tag{3}$$

For planar rods $\tau = 0$, and for straight rods $\chi = \tau = 0$.

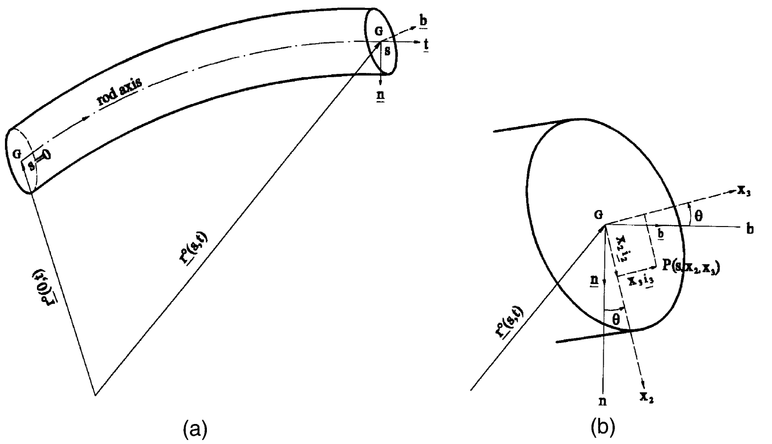


Fig. 1. The rod geometry.

A second rectangular frame $(x_1, x_2, x_3)$ is introduced such that the $x_1$-axis is in the direction of **t**, and $x_2$, $x_3$ axes are the principal axes of the cross-section (Fig. 1b). Let $\mathbf{i}_1$, $\mathbf{i}_2$ and $\mathbf{i}_3$ be the unit vectors along $x_1$, $x_2$, $x_3$. From Fig. 1b Eq. (4) can be written.

$$\mathbf{t} = \mathbf{i}_1, \quad \mathbf{n} = \mathbf{i}_2 \cos\theta - \mathbf{i}_3 \sin\theta, \quad \mathbf{b} = \mathbf{i}_2 \sin\theta + \mathbf{i}_3 \cos\theta \tag{4}$$

## 3. Governing equations

Let the displacement of a point on the rod axis, and the rotation of the cross-section about an axis passing through $G$ be denoted by $\mathbf{U}^0(s,t)$ and $\mathbf{\Omega}^0(s,t)$, respectively. Also, let $\boldsymbol{\gamma}^0(s,t)$ and $\boldsymbol{\omega}^0(s,t)$, stand for extension and rotation of the unit length on the rod axis, respectively.

On the other hand, let $\mathbf{T}(s,t)$ and $\mathbf{M}(s,t)$ denote, respectively, the resultant of the internal stresses acting on the cross-section, and the resultant moment obtained when $\mathbf{T}(s,t)$ is carried to the geometric center $G$. Also let $\mathbf{p}^{\mathrm{ex}}(s,t)$ and $\mathbf{m}^{\mathrm{ex}}(s,t)$ be the external distributed load and moment per unit length of the rod axis.

Assuming infinitesimal deformations, the equations of geometric compatibility and the equations of motion are, respectively, given by Kıral and Ertepınar (1974).

$$\boldsymbol{\gamma}^0 = \frac{\partial \mathbf{U}^0}{\partial s} + \mathbf{t} \times \mathbf{\Omega}^0, \qquad \boldsymbol{\omega}^0 = \frac{\partial \mathbf{\Omega}^0}{\partial s} \tag{5}$$

$$\frac{\partial \mathbf{T}^0}{\partial s} + \mathbf{p}^{(\mathrm{ex})} = \mathbf{p}^{(\mathrm{in})}, \qquad \frac{\partial \mathbf{M}^0}{\partial s} + \mathbf{t} \times \mathbf{T}^0 + \mathbf{m}^{(\mathrm{ex})} = \mathbf{m}^{(\mathrm{in})} \tag{6}$$

The components along the $x_1$, $x_2$ and $x_3$ axes of the inertia force and moment $\mathbf{p}^{\mathrm{in}}$ and $\mathbf{m}^{\mathrm{in}}$ are defined as

$$p_i^{(\mathrm{in})} = -\rho A \frac{\partial^2 U_i^0}{\partial t^2}, \quad m_i^{(\mathrm{in})} = -\rho I_i \frac{\partial^2 \Omega_i^0}{\partial t^2} \qquad (i = 1,2,3) \tag{7}$$

where $\rho$ is the mass density.

The relevant components of the strain tensor $e_{ij}$ in the $x_i$-frame are obtained in terms of relative extension $\gamma^0$ and rotation $\omega^0$ as (see Kıral et al., 1976)

$$\begin{aligned} e_{11} &= \gamma_1^0 - x_2\omega_3^0 + x_3\omega_2^0 \\ e_{12} &= \tfrac{1}{2}(\gamma_2^0 - x_3\omega_1^0) \\ e_{13} &= \tfrac{1}{2}(\gamma_3^0 + x_2\omega_1^0) \\ e_{23} &\cong 0 \end{aligned} \tag{8}$$

Equations of geometric compatibility and equations of motion are derived under the assumption that the displacements and their gradients are infinitesimal. Further, it is assumed that the largest dimension of the cross-section is small compared to the radii of curvature and the twist of the rod axis. Also, the effect of warping of the cross-section is ignored.

The equations of geometric compatibility (5) and the equations of motion (6) are valid irrespective of the constitution of the rod material. Thus, there are four vectorial equations in six vectorial unknowns, namely, $\mathbf{U}^0$, $\mathbf{\Omega}^0$, $\mathbf{T}^0$, $\mathbf{M}^0$, $\boldsymbol{\gamma}^0$ and $\boldsymbol{\omega}^0$. The remaining two equations necessary for the determination of these unknowns are the constitutive equations.

The nature of the rod material is brought into the formula to make it adequate for the determination of these unknowns. The material of the rod is homogeneous, isotropic and linearly viscoelastic. For later use, it is further assumed that there exists an initial state $t = 0$ for which the body is stress free. Since the rod under consideration is slender, the usual assumptions on the stresses

$$\sigma_{22} = \sigma_{33} = 0 \tag{9}$$

are imposed.

## 4. Constitutive equations in integral form

Constitutive equations in integral or differential forms and the interrelation between them can be found in Eringen (1982). An equivalent stress constitutive equation of the Boltzmann–Volterra theory, in terms of deviatoric and dilatational parts of the strain is

$$\sigma_{ij} = \delta_{ij} \int_0^t K(t-\tau) \frac{\partial e_{rr}(\tau)}{\partial \tau} \, \mathrm{d}\tau + 2 \int_0^t G(t-\tau) \frac{\partial e'_{ij}(\tau)}{\partial \tau} \, \mathrm{d}\tau \tag{10}$$

where the deviatoric strain components $e'_{ij}$ are defined by

$$e'_{ij} = e_{ij} - \tfrac{1}{3} e_{rr} \delta_{ij} \tag{11}$$

in which $e_{rr} = e_{11} + e_{22} + e_{33}$. The memory function $K(t)$ and $G(t)$ in (10) are named relation bulk modulus and shear modulus, respectively.

The remaining components $\bar{\sigma}_{11}$, $\bar{\sigma}_{12}$, $\bar{\sigma}_{13}$ and $\bar{\sigma}_{23}$ of the transformed stress tensor are then obtained by taking Laplace transform of (10), making use of the constraining condition (9) and noting that $e'_{ii} = 0$. They are

$$\bar{\sigma}_{11} = z\overline{E}\bar{e}_{11}, \quad \bar{\sigma}_{12} = 2z\overline{G}\bar{e}_{12}, \quad \bar{\sigma}_{13} = 2z\overline{G}\bar{e}_{13}, \quad \bar{\sigma}_{23} = 0 \tag{12}$$

where $z$ is the Laplace transform parameter, and the relaxation Young's modulus $E(t)$ and the Poisson's ratio $\upsilon(t)$, in the transform domain, are defined by

$$\overline{E} = \frac{9\overline{K}\,\overline{G}}{3\overline{K} + \overline{G}}, \qquad \bar{\upsilon} = \frac{3\overline{K} - 2\overline{G}}{6\overline{K} + 2\overline{G}} \tag{13}$$

Note that the inverse Laplace transformation of Eqs. (12), with the help of convolution theorem in Spiegel (1965), yields

$$\begin{aligned}
\sigma_{11} &= \int_0^t E(t-\tau) \frac{\partial e_{11}(\tau)}{\partial \tau} \mathrm{d}\tau \\
\sigma_{12} &= 2\int_0^t G(t-\tau) \frac{\partial e_{12}(\tau)}{\partial \tau} \mathrm{d}\tau \\
\sigma_{13} &= 2\int_0^t G(t-\tau) \frac{\partial e_{13}(\tau)}{\partial \tau} \mathrm{d}\tau \\
\sigma_{22} &= \sigma_{33} = \sigma_{23} = 0
\end{aligned} \tag{14}$$

The components in $x_i$—rectangular Cartesian frame of the stress resultants $\mathbf{T}(s,t)$ and moment resultants $\mathbf{M}(s,t)$ are expressed in terms of the stresses on the cross-section as

$$T_i = \int_A \sigma_{1i} \, \mathrm{d}A \quad (i = 1, 2, 3) \tag{15}$$

$$M_1 = \int_A (x_2\sigma_{13} - x_3\sigma_{12})\,\mathrm{d}A$$
$$M_2 = \int_A x_3\sigma_{11}\,\mathrm{d}A \tag{16}$$
$$M_3 = -\int_A x_2\sigma_{11}\,\mathrm{d}A$$

where $A$ is area of the cross-section considered. After taking the Laplace transform of Eqs. (15), (16) and (8), in variable $t$, and substituting (11) in (12), then a subsequent substitution of the resulting equation into (15) and (16) yield the resultant constitutive equations in the transform domain as

$$\overline{T}_1 = z\overline{E}A\bar{\gamma}_1^0, \quad \overline{T}_2 = z\overline{G}A\bar{\gamma}_2^0, \quad \overline{T}_3 = z\overline{G}A\bar{\gamma}_3^0 \tag{17}$$

$$\overline{M}_1 = z\overline{G}I_1\bar{\omega}_1^0, \quad \overline{M}_2 = z\overline{E}I_2\bar{\omega}_2^0, \quad \overline{M}_3 = z\overline{E}I_3\bar{\omega}_3^0 \tag{18}$$

Note that, by comparing Eqs. (17) and (18) with the corresponding elasticity equations, the transformed viscoelastic resultant constitutive equations may be obtained directly by replacing the Young's modulus $E$ by $z\overline{E}$ and shear modulus $G$ by $z\overline{G}$. Also note that, the inverse transform of Eqs. (17) and (18), if they exist, with the use of convolution theorem, are given by

$$T_1 = A\int_0^t E(t-\tau)\frac{\partial\gamma_1^0}{\partial\tau}\mathrm{d}\tau, \quad T_i = A\int_0^t G(t-\tau)\frac{\partial\gamma_i^0}{\partial\tau}\mathrm{d}\tau \quad (i = 2,3) \tag{19}$$

$$M_1 = I_1\int_0^t G(t-\tau)\frac{\partial\omega_1^0}{\partial\tau}\mathrm{d}\tau, \quad M_i = I_i\int_0^t E(t-\tau)\frac{\partial\omega_i^0}{\partial\tau}\mathrm{d}\tau \quad (i = 2,3) \tag{20}$$

which are the resultant constitutive equations in the time domain.

## 5. Laplace transforms of the governing equations

For the case of forced vibrations, a column matrix $\mathbf{Y}(s,t)$ is introduced as

$$\mathbf{Y}(s,t) = \{U_1^0, U_2^0, U_3^0, \Omega_1^0, \Omega_2^0, \Omega_3^0, T_1^0, T_2^0, T_3^0, M_1^0, M_2^0, M_3^0\}^{\mathrm{T}} \tag{21}$$

Laplace transform of Eq. (21) with respect to time is

$$\overline{\mathbf{Y}}(s,z) = L[\mathbf{Y}(s,t)] \tag{22}$$

where Laplace transform parameter $z$ is a complex number. With the aid of these definitions, Eqs. (5) and (6) are reduced to a set of 12 first order non-homogeneous ordinary differential equations

$$\frac{\mathrm{d}\overline{\mathbf{Y}}(s,z)}{\mathrm{d}s} = \overline{\mathbf{F}}(s,z)\overline{\mathbf{Y}}(s,z) + \overline{\mathbf{B}}(s,z) \tag{23}$$

Some of the elements of $\overline{\mathbf{F}}(s,z)$ are obtained by applying Laplace transform of the following second derivatives

$$\begin{aligned} L\left[\rho A\frac{\partial^2 U_k^0}{\partial t^2}\right] &= \rho A\left[z^2\overline{U}_k^0 - zU_k^0(s,0) - \frac{\partial U_k^0(s,0)}{\partial t}\right] \\ L\left[\rho I_k\frac{\partial^2 \Omega_k^0}{\partial t^2}\right] &= \rho I_k\left[z^2\bar{\Omega}_k^0 - z\Omega_k^0(s,0) - \frac{\partial \Omega_k^0(s,0)}{\partial t}\right] \end{aligned} \quad (k = 1,2,3) \tag{24}$$

The second and third terms on the right-hand side of Eq. (24) are the initial conditions given at $t = 0$. The elements of the column matrix $\overline{\mathbf{B}}(s,z)$ are

$$\overline{B}_i(s,z) = 0 \quad (i = 1,2,\ldots,6)$$
$$\overline{B}_{6+j}(s,z) = -(\bar{p}_k^{(\mathrm{ex})}) - \rho A\left[zU_k^0(s,0) + \frac{\partial U_k^0(s,0)}{\partial t}\right] \quad (j = 1,2,3)$$
$$\overline{B}_{9+j}(s,z) = -(\bar{m}_k^{(\mathrm{ex})}) - \rho I_k\left[z\Omega_k^0(s,0) + \frac{\partial \Omega_k^0(s,0)}{\partial t}\right] \quad (k = 1,2,3) \tag{25}$$

Note that the initial conditions present in Eqs. (24) are now included in the load vector $\overline{\mathbf{B}}(s,z)$.

## 6. Special cases

The spatially curved system is taken as a special case of a helical bar. The parametric equation of a helix is given by Temel and Çalım (2003) (see Fig. 2)

$$x = a\cos\phi, \quad y = a\sin\phi, \quad z = h\phi \tag{26}$$

where $\phi$ is the horizontal angle of the helix. The infinitesimal length element of the helix is defined as

$$c = \sqrt{a^2 + h^2}, \quad \mathrm{d}s = c\,\mathrm{d}\phi, \quad \cos\alpha = \frac{a}{c}, \quad \sin\alpha = \frac{h}{c} \tag{27}$$

where $\alpha$ and $a$ are pitch angle and centerline radius of the helix, respectively. The curvatures of a cylindrical helical spring are

$$\chi = \frac{a}{c^2} = \text{constant}, \qquad \tau = \frac{h}{c^2} = \text{constant} \tag{28}$$

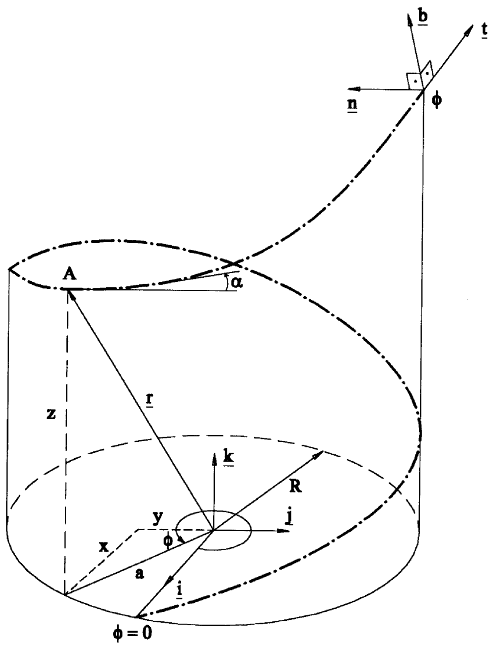


Fig. 2. Geometry of a cylindrical helix.

The relationship between the moving axis $(\mathbf{t},\mathbf{n},\mathbf{b})$ and the fixed reference frame $(\mathbf{i},\mathbf{j},\mathbf{k})$ are (Fig. 2)

$$\{V\}^{\mathrm{T}}_{tnb}=[B]\{V\}^{\mathrm{T}}_{ijk}\quad \begin{Bmatrix} V_t \\ V_n \\ V_b \end{Bmatrix}=\begin{bmatrix} -(a/c)\sin\phi & (a/c)\cos\phi & (h/c) \\ -\cos\phi & -\sin\phi & 0 \\ (h/c)\sin\phi & -(h/c)\cos\phi & (a/c) \end{bmatrix}\begin{Bmatrix} V_i \\ V_j \\ V_k \end{Bmatrix} \tag{29}$$

Non-dimensional parameters in Laplace domain are defined as

$$\overline{U}_i=\frac{1}{c}U^0_i,\quad \overline{\Omega}_i=\Omega^0_i,\quad \overline{T}_i=\frac{c^2}{EI_n}T^0_i,\quad \overline{M}_i=\frac{c}{EI_n}M^0_i\qquad (i=t,n,b) \tag{30}$$

Assuming that the centroid and the shear center of cross-section coincide, the **n**, **b** axes become the principal axes and the effect of warping of the cross-section is ignored. Now, equations obtained as a result of elimination of $\boldsymbol{\gamma}^0$ and $\boldsymbol{\omega}^0$ between the transformed equations of compatibility (5) and the transformed constitutive equations (17) and (18) together with the transformed equations of motion (6) form the governing equations of the dynamic response of initially curved and twisted viscoelastic bars. Finally, using Eqs. (27), (28), (30), the governing equations in canonical form are given as follows

$$\frac{\mathrm{d}\overline{U}_t}{\mathrm{d}\phi}=\frac{a}{c}\overline{U}_n+\frac{EI_n}{z\overline{E}Ac^2}\overline{T}_t \tag{31a}$$

$$\frac{\mathrm{d}\overline{U}_n}{\mathrm{d}\phi}=-\frac{a}{c}\overline{U}_t+\frac{h}{c}\overline{U}_b+\overline{\Omega}_b+\frac{\alpha_nEI_n}{z\overline{G}Ac^2}\overline{T}_n \tag{31b}$$

$$\frac{\mathrm{d}\overline{U}_b}{\mathrm{d}\phi}=-\frac{h}{c}\overline{U}_n-\overline{\Omega}_n+\frac{\alpha_bEI_n}{z\overline{G}Ac^2}\overline{T}_b \tag{31c}$$

$$\frac{\mathrm{d}\overline{\Omega}_t}{\mathrm{d}\phi}=\frac{a}{c}\overline{\Omega}_n+\frac{EI_n}{z\overline{G}I_t}\overline{M}_t \tag{31d}$$

$$\frac{\mathrm{d}\overline{\Omega}_n}{\mathrm{d}\phi}=-\frac{a}{c}\overline{\Omega}_t+\frac{h}{c}\overline{\Omega}_b+\frac{E}{z\overline{E}}\overline{M}_n \tag{31e}$$

$$\frac{\mathrm{d}\overline{\Omega}_b}{\mathrm{d}\phi}=-\frac{h}{c}\overline{\Omega}_n+\frac{EI_n}{z\overline{E}I_b}\overline{M}_b \tag{31f}$$

$$\frac{\mathrm{d}\overline{T}_t}{\mathrm{d}\phi}=\frac{\rho Ac^4z^2}{EI_n}\overline{U}_t+\frac{a}{c}\overline{T}_n+\overline{B}_7 \tag{31g}$$

$$\frac{\mathrm{d}\overline{T}_n}{\mathrm{d}\phi}=\frac{\rho Ac^4z^2}{EI_n}\overline{U}_n-\frac{a}{c}\overline{T}_t+\frac{h}{c}\overline{T}_b+\overline{B}_8 \tag{31h}$$

$$\frac{\mathrm{d}\overline{T}_b}{\mathrm{d}\phi}=\frac{\rho Ac^4z^2}{EI_n}\overline{U}_b-\frac{h}{c}\overline{T}_n+\overline{B}_9 \tag{31i}$$

$$\frac{\mathrm{d}\overline{M}_t}{\mathrm{d}\phi}=\frac{\rho I_tc^2z^2}{EI_n}\overline{\Omega}_t+\frac{a}{c}\overline{M}_n+\overline{B}_{10} \tag{31j}$$

$$\frac{\mathrm{d}\overline{M}_n}{\mathrm{d}\phi}=\frac{\rho c^2z^2}{E}\overline{\Omega}_n+\overline{T}_b-\frac{a}{c}\overline{M}_t+\frac{h}{c}\overline{M}_b+\overline{B}_{11} \tag{31k}$$

$$\frac{\mathrm{d}\overline{M}_b}{\mathrm{d}\phi} = \frac{\rho I_b c^2 z^2}{EI_n}\overline{\Omega}_b - \overline{T}_n - \frac{h}{c}\overline{M}_n + \overline{B}_{12} \tag{31l}$$

Irrespective of the rod geometry, the following four cases may now be distinguished,

Case 1: static loading, elastic material,
Case 2: static loading, viscoelastic material (quasi-static case),
Case 3: dynamic loading, elastic material,
Case 4: dynamic loading, viscoelastic material.

In the cases of static loading, the terms including mass density in Eqs. (31g)–(31l) become null, irrespective of the rod material being elastic or viscoelastic. When the rod material is viscoelastic, the Young's modulus $E$ and shear modulus $G$ is replaced by $z\overline{E}$ and $z\overline{G}$.

## 7. Solutions of the differential equations with the complementary functions method

Eqs. (31a)–(31l) make up a set of 12 simultaneous differential equations with constant coefficients. Each one of these equations involves first-order derivatives with respect to position. The relationships given for the dynamic loading case in the Laplace space in Temel and Çalım (2003) are modified to be used for the viscoelastic material cases. In matrix notation, Eqs. (31a)–(31l) can be expressed as

$$\frac{\mathrm{d}\overline{\mathbf{Y}}(\phi,z)}{\mathrm{d}\phi} = \overline{\mathbf{F}}(\phi,z)\overline{\mathbf{Y}}(\phi,z) + \overline{\mathbf{B}}(\phi,z) \tag{32}$$

For the case of spatial bar, the elements of state vector are defined as

$$\overline{\mathbf{Y}}(\phi,z) = \{\overline{\mathbf{U}}(\phi,z), \overline{\mathbf{\Omega}}(\phi,z), \overline{\mathbf{T}}(\phi,z), \overline{\mathbf{M}}(\phi,z)\}^{\mathrm{T}} \tag{33}$$

The complementary functions method is based on the principle of solving Eq. (33) with the aid of initial conditions. This method is basically the reduction of two-point boundary value problems to the numerical solution of initial-value problems which are much more suitable for programming. The general solution of Eq. (33), is given by

$$\overline{\mathbf{Y}}(\phi,z) = \sum_{m=1}^{12} C_m(\overline{\mathbf{U}}^{(m)}(\phi,z)) + \overline{\mathbf{V}}(\phi,z) \tag{34}$$

where $\overline{\mathbf{U}}^{(m)}(\phi,z)$ is the complementary solution such that its $m$th component is equal to 1, whereas all the others are 0. $\overline{\mathbf{V}}(\phi,z)$ is the inhomogeneous solution with all 0 initial conditions, the integration constants $C_m$ will be determined from the boundary conditions at both ends.

## 8. Determination of the dynamic stiffness matrix

The element equation is given in the Laplace domain by

$$\{\bar{p}\} = [\bar{k}]\{\bar{d}\} + \{\bar{f}\} \tag{35}$$

There are six degrees of freedom at each node, three of these six are translations and others are rotations. Letting $i$ stand for the beginning and $j$ for the end of an element, the end displacements and the end forces are given as

$$\{\bar{d}\}^{\mathrm{T}} = \{\overline{\mathbf{U}}(\phi_i, z), \overline{\mathbf{\Omega}}(\phi_i, z), \overline{\mathbf{U}}(\phi_j, z), \overline{\mathbf{\Omega}}(\phi_j, z)\} \tag{36}$$

$$\{\bar{p}\}^{\mathrm{T}} = \{\overline{\mathbf{T}}(\phi_i, z), \overline{\mathbf{M}}(\phi_i, z), \overline{\mathbf{T}}(\phi_j, z), \overline{\mathbf{M}}(\phi_j, z)\} \tag{37}$$

In order to determine the element stiffness matrix, the end displacements of the element as defined in (36) are equated to unity for any one of the 12 directions while keeping the others 0. This is done 12 times using each equation. From the homogeneous solution of the system (31), the element end forces are obtained, and these forces are incorporated into the element dynamic stiffness matrix.

The fixed-end forces are computed from (31) by taking all the end displacements to be equal to 0 as

$$\{\bar{f}\}^{\mathrm{T}} = \{-\overline{\mathbf{T}}(\phi_i, z), -\overline{\mathbf{M}}(\phi_i, z), \overline{\mathbf{T}}(\phi_j, z), \overline{\mathbf{M}}(\phi_j, z)\} \tag{38}$$

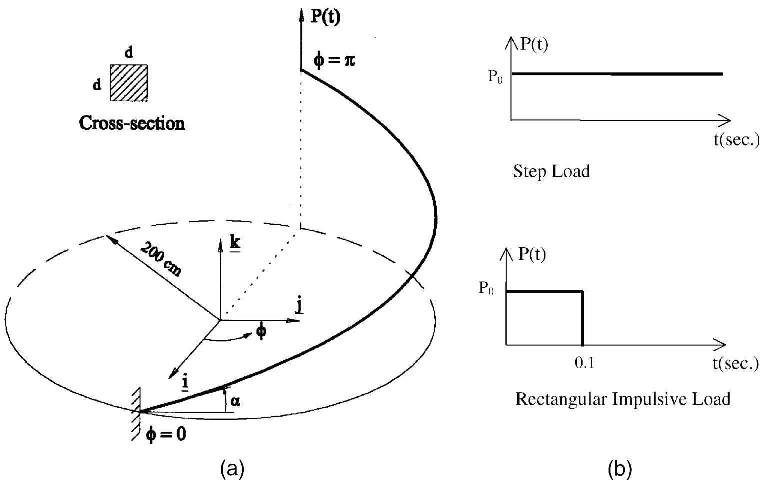


Fig. 3. (a) A cantilever helical rod; (b) type of dynamic loads.

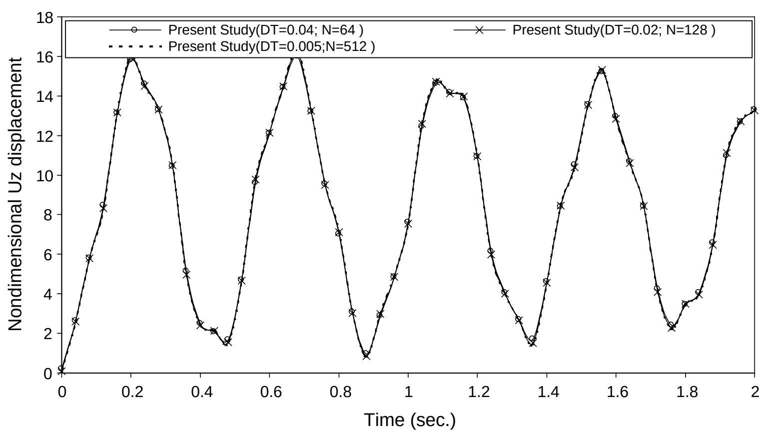


Fig. 4. Vertical displacement versus time at the free end for step load.

For the transformation to the common reference system, the following equations are used

$$\lfloor \bar{k} \rfloor_{ijk} = [T]^{\mathrm{T}} \lfloor \bar{k} \rfloor_{tnb} [T] \tag{39}$$

$$\{\bar{f}\}_{ijk} = [T]^{\mathrm{T}} \{\bar{f}\}_{tnb} \tag{40}$$

where the transformation matrix $[T]$ is given by

$$[T] = \begin{bmatrix} [B(\phi_i)] & [0] & [0] & [0] \\ [0] & [B(\phi_i)] & [0] & [0] \\ [0] & [0] & [B(\phi_j)] & [0] \\ [0] & [0] & [0] & [B(\phi_j)] \end{bmatrix}_{12\times 12} \tag{41}$$

and $[B]$ is defined in Eq. (29).

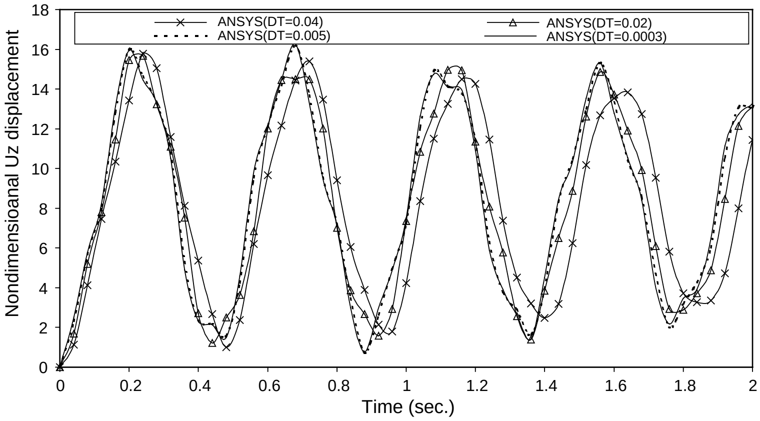


Fig. 5. Vertical displacement versus time at the free end for step load.

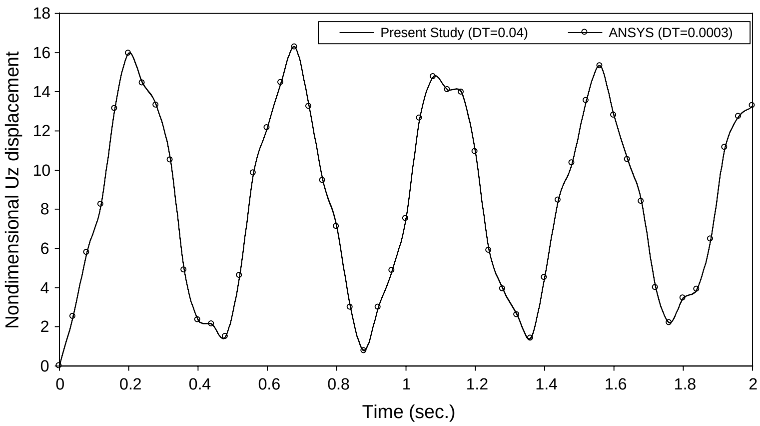


Fig. 6. Vertical displacement versus time at the free end for step load.

In this study, both the element dynamic stiffness matrix $\lfloor \bar{k} \rfloor$ and the fixed-end forces $\{\bar{f}\}$ are determined by solving Eq. (31) by the complementary functions method in the Laplace domain. The system of equations of motion can then be assembled from the element dynamic stiffness matrices and end forces as

$$[\mathbf{K}(\mathbf{z})]\{\mathbf{D}\} = \{\mathbf{P}(\mathbf{z})\} \tag{42}$$

where $[\mathbf{K}(\mathbf{z})]$ and $\{\mathbf{P}(\mathbf{z})\}$ are the system dynamic stiffness matrix and the load vector. $\{\mathbf{D}\}$ is the vector of unknown displacements of the system.

## 9. Verification of the proposed model

An elastic cantilever helical rod shown in Fig. 3 is analyzed first to determine the effect of time increment and Laplace transform parameter. The vertical displacement of the free end under a step load is presented in Fig. 4. It is obvious that results obtained using a coarse time increment ($DT = 0.04$) along with fewer Laplace transform parameter overlap exactly the results obtained using finer increments and higher parameters which indicates the efficiency of the present model. Fig. 5 shows the displacement results ob-

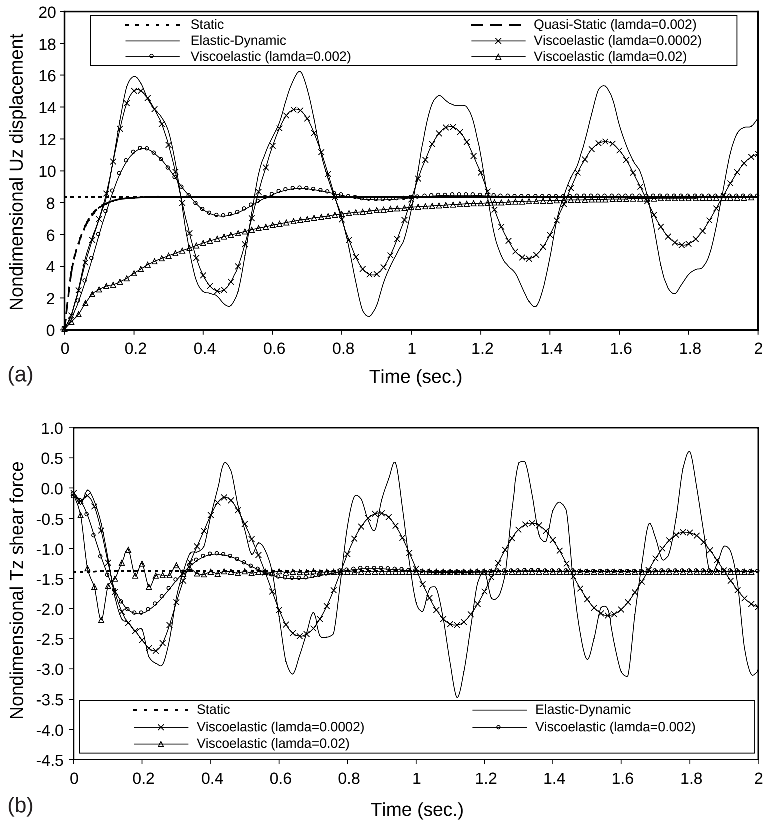


Fig. 7. (a) Vertical displacement versus time at the free end for step load. (b) Vertical shear force versus time at the fixed end for step load. (c) *My* moment versus time at the fixed end for step load. (d) *Mz* moment versus time at the fixed end for step load.

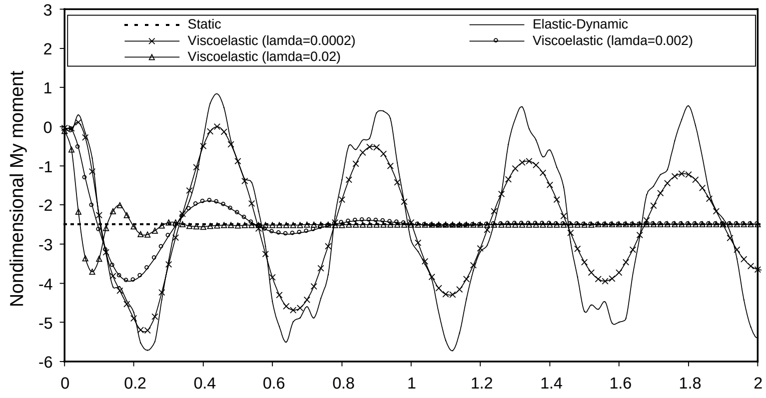

(c)

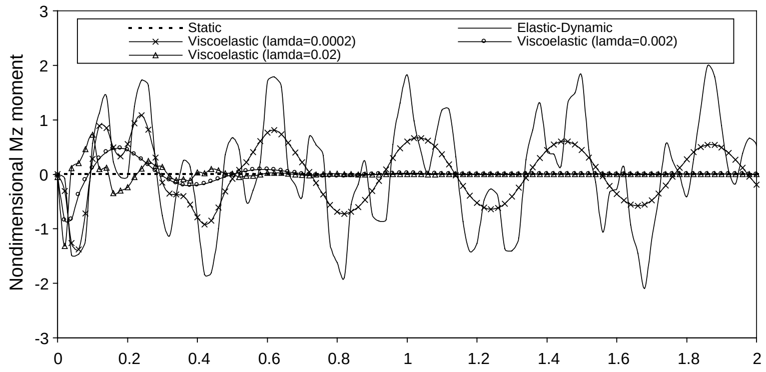

(d)

Fig. 7 (*continued*)

tained via the finite element program ANSYS [1] using 81 straight-beam elements. It can be seen that time increments of 0.005 and finer had to be considered for consistent results. The comparison of proposed model with ANSYS is done in Fig. 6. An exact match is obtained by using a single element and a time increment of 0.04 in the present model as opposed to 81 elements and much finer increment of 0.0003 in ANSYS. The material and geometric properties used are: $d = 12$ cm, $\alpha = 25.52°$, $a = 200$ cm, $E = 2.06 \times 10^{11}$ N/m$^2$, $\rho = 7850$ kg/m$^3$ and $\nu = 0.3$.

## 10. Numerical example

In this study, a general-purpose computer program is coded in FORTRAN77 for time-dependent loads to analyse quasi-static and dynamic response of cylindrical helical rods made of linear viscoelastic materials. Butcher's fifth-order Runge–Kutta algorithm in Chapra and Canale (1998) is used for the solution of the initial-value problem based on the complementary function method. Forty steps of integration are used

[1] ANSYS Swanson Analysis System, Inc., 201 Johnson Road, Houston, PA 15342-1300, USA.

in the analysis. The Durbin's inverse Laplace transform (see Appendix A, Durbin, 1974; Narayanan, 1979) is applied for transformation from the Laplace domain to the time domain.

The viscoelastic characteristics of the rod material is denoted in the form by Kıral et al. (1976)

$$G(t) = G_0[1 + B\mathrm{Exp}(-t/\lambda)], \qquad K(t) = K_0 \tag{43}$$

with their Laplace transforms

$$\overline{G}(z) = G_0\left(\frac{1}{z} + \frac{B}{z + \frac{1}{\lambda}}\right), \qquad \overline{K}(z) = \frac{K_0}{z} \tag{44}$$

where $\lambda$ (lambda) is the relaxation time, $G_0$ is the elastic shear constant, $K_0$ is the elastic bulk modulus and $B = 20$.

**Example 1.** A cantilever helical rod is now considered. The parameters used in this example are those used by Temel and Çalım (2003) for the elastic material. Various dynamic loads are applied on the free end of the rod. Material and geometrical properties are: $d = 12$ cm, $\alpha = 25.52°$, $a = 200$ cm, $E = 2.06 \times 10^{11}$ N/m$^2$,

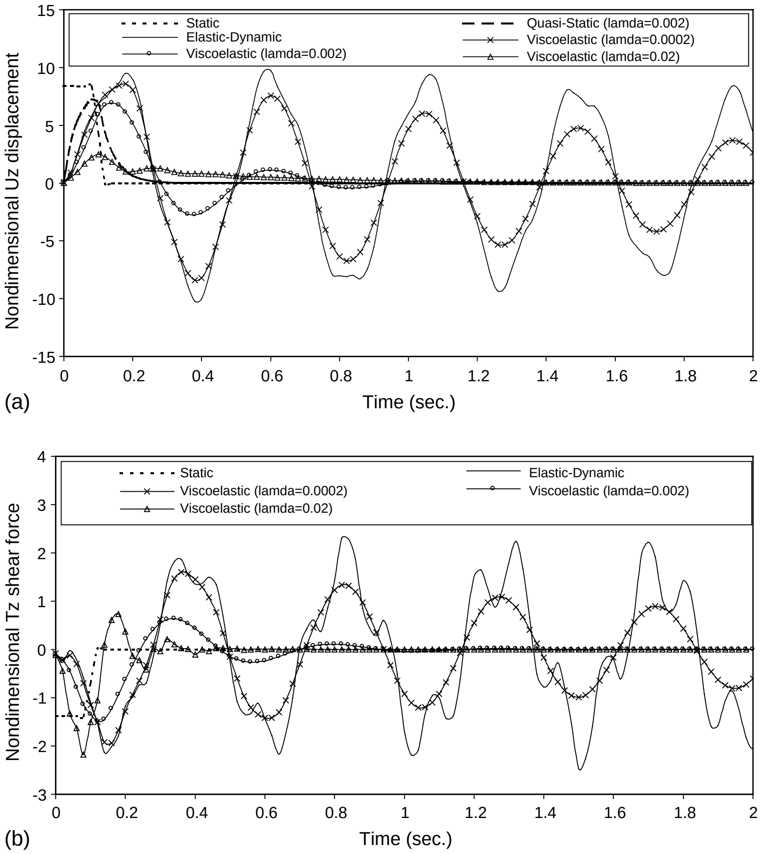


Fig. 8. (a) Vertical displacement versus time at the free end for rectangular impulsive load. (b) Vertical shear force versus time at the fixed end for rectangular impulsive load. (c) *My* moment versus time at the fixed end for rectangular impulsive load. (d) *Mz* moment versus time at the fixed end for rectangular impulsive load.

$\rho = 7850$ kg/m$^3$ and $\nu = 0.3$ (see Fig. 3). Various dynamic loads with the amplitude $P_0 = 10^6$ N are applied vertically at the free end of the rod. A time increment $\Delta t$ of 0.02 s is used in the calculations.

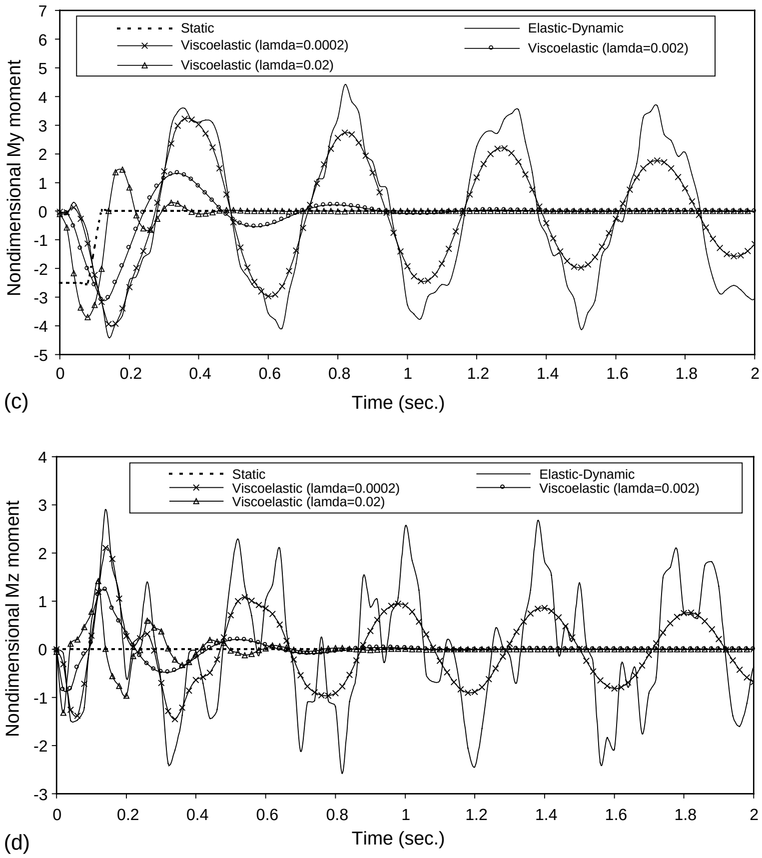


Fig. 8 (*continued*)

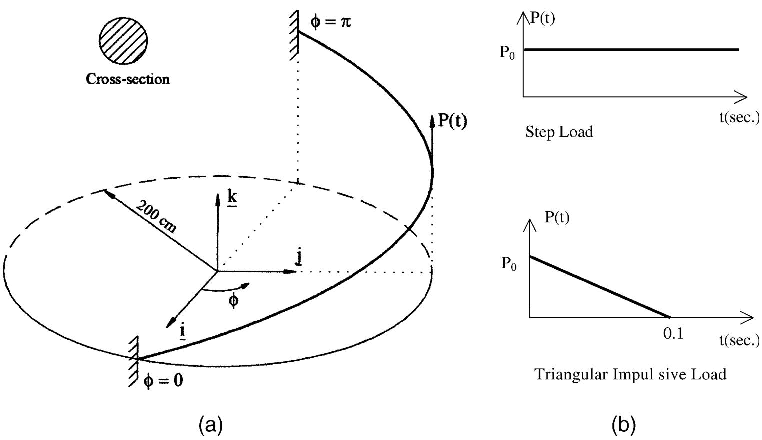


Fig. 9. (a) A fixed-ended helical rod; (b) type of dynamic loads.

Non-dimensional vertical displacement at the free end and non-dimensional shear force, bending moment at the fixed end are shown in Figs. 7a–d and 8a–d for different loading cases.

The figures include, static, elastic–dynamic, quasi-static and viscoelastic cases for various damping ratios. As expected, the elastic–dynamic response oscillates about the static state. The quasi-static response approaches the static state with time. In the viscoelastic case, the response of the bar dies out with time. The effect of the damping ratio is obvious; increasing the damping ratio causes the response to reach the static response much faster.

The dynamic behaviour of the viscoelastic helical bar will eventually disappear and it will approach the static state. The moment *Mz* is equal to 0 under static loads. However, in the case of dynamic loads, due to inertia forces it assumes values different from 0 (see Figs. 7d and 8d).

**Example 2.** A fixed-ended helical rod shown in Fig. 9 is now considered. The rod has a circular cross-section with the diameter $d = 12$ cm. The pitch angle and radius of the helix circle are chosen as $\alpha = 25.52°$ and $a = 200$ cm, respectively. Material properties are: $E = 2.06 \times 10^{11}$ N/m$^2$, $\rho = 7850$ kg/m$^3$ and $\nu = 0.3$. Various dynamic loads with the amplitude $P_0 = 5 \times 10^5$ N are applied vertically on the arc-length mid-point of the rod. A time increment $\Delta t$ of 0.02 s is used in the calculations.

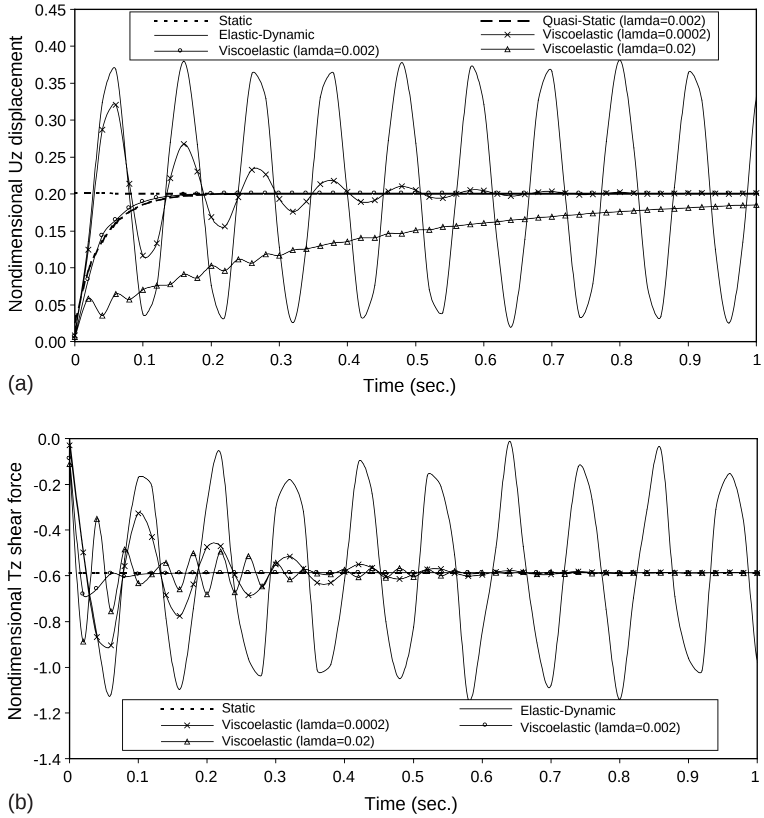


Fig. 10. (a) Vertical displacement versus time at the arc-length mid-point for step load. (b) Vertical shear force versus time at the fixed end for step load. (c) *My* moment versus time at the fixed end for step load. (d) *Mz* moment versus time at the fixed end for step load.

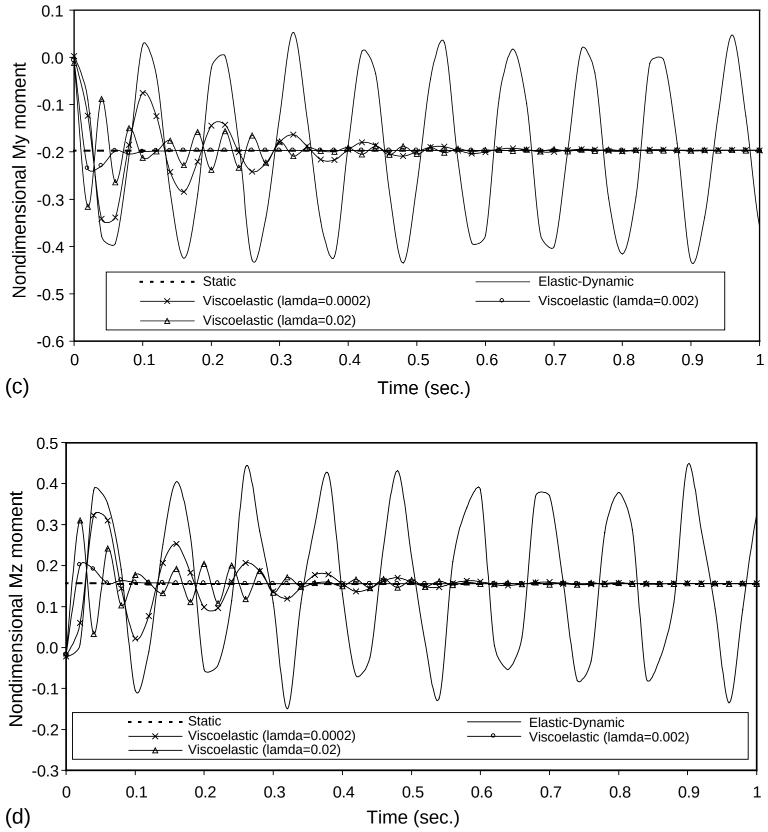


Fig. 10 (*continued*)

Non-dimensional vertical displacement at the arc-length mid-point of the rod and non-dimensional shear force, bending moments at the fixed end are shown in Figs. 10a–d and 11a–d for different loading cases.

The conclusions derived from the previous example can be reiterated here in that the dynamic behaviour of the viscoelastic helical bar will also eventually disappear and it will approach its the static state. It should be emphasized again that the aim of the present work is to demonstrate the application of an efficient method to the viscoelastic case rather than reconfirming the expected viscoelestic response of helical bars.

## 11. Discussions and conclusions

The quasi-static and dynamic response of cylindrical helical rods made of linear viscoelastic materials are investigated using an efficient method of analysis in the Laplace domain in this study.

The dynamic stiffness matrix has been calculated in the Laplace domain by applying the complementary functions method to the differential equations in canonical form. This provides great convenience in the solution of the physical problems having general boundary conditions. Another advantage of using the complementary functions method-based solution is that the helical rods with variable cross-section and geometry, which yield ordinary differential equations having variable coefficients, can also be considered.

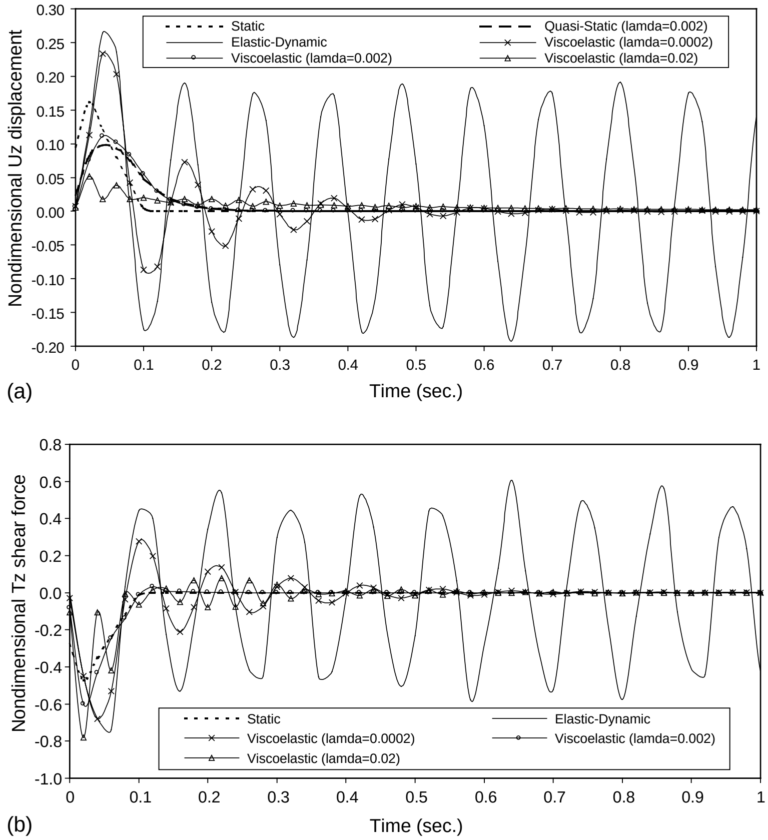


Fig. 11. (a) Vertical displacement versus time at the arc-length mid-point for triangular impulsive load. (b) Vertical shear force versus time at the fixed end for triangular impulsive load. (c) *My* moment versus time at the fixed end for triangular impulsive load. (d) *Mz* moment versus time at the fixed end for triangular impulsive load.

The differential equations can be solved by using the complementary functions method with sufficient accuracy as required with an appropriate integration step-size.

The quasi-static and dynamic behaviour of cylindrical helical rods are investigated by using the Boltzmann–Volterra theory for viscoelastic materials. The dynamic behaviour of the viscoelastic helical bar will disappear after some time, approaching the static state. The time to reach the static behaviour is proportional to the damping coefficient. The damping effects in viscoelastic material reduce the peak values of the dynamic response.

## Appendix A. Modified durbin's inverse Laplace transform method

A numerical inverse Laplace transform technique is necessary to obtain the values in the time domain. For this purpose, Durbin's inverse Laplace transform technique based on the fast Fourier transform (FFT) is used by Durbin (1974). Durbin's formulation for inverse Laplace transform is summarized as follows:

$$f(t_j) \cong \frac{2e^{aj\,\Delta t}}{T}\left[-\frac{1}{2}\mathrm{Re}\{\overline{F}(a)\} + \mathrm{Re}\left\{\sum_{k=0}^{N-1}(\overline{F}(z_k)L_k)e^{\left(i\frac{2\pi}{N}\right)jk}\right\}\right] \quad (j = 0, 1, 2, \ldots, N-1) \tag{A.1}$$

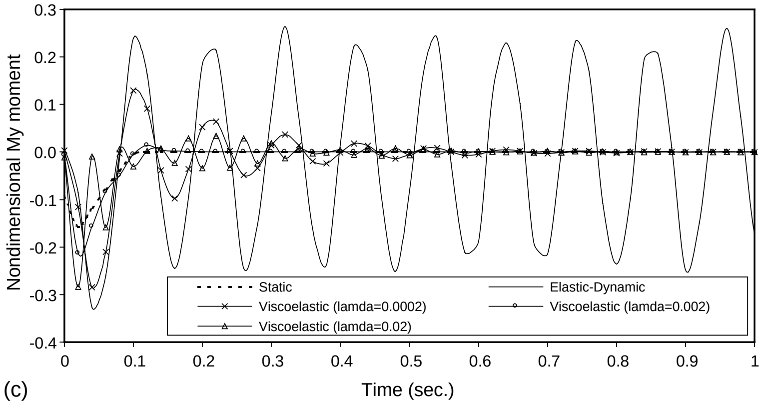

(c)

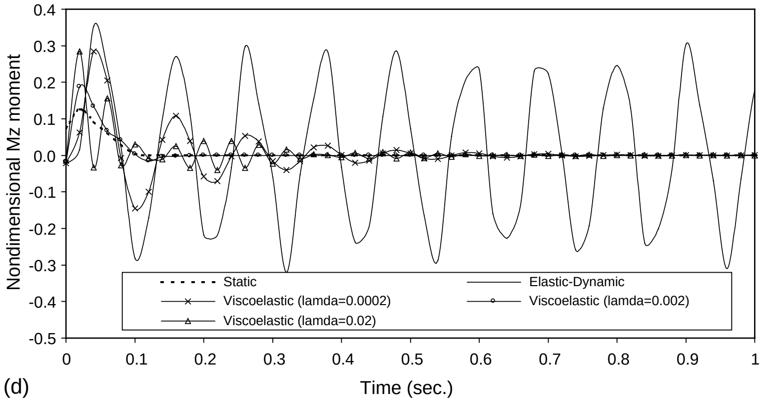

(d)

Fig. 11 (*continued*)

in which $z_k = a + \mathrm{i}k\frac{2\pi}{T}$, $N = T/\Delta t$ where $z_k$ is the $k$th Laplace transform parameter, $T$ is the solution interval and $\Delta t$ is the time increment. The selection of constant '$a$' in numerical inverse Laplace transforms is explained in Durbin (1974). It is implied that if the value of '$aT$' is chosen in the range 5–10, good results are obtained. Therefore, for the numerical examples presented in this paper the value of '$aT$' is generally taken as '6'. Finally, results can be modified by multiplying each term Lanczos ($L_k$) factors to obtain better results in the Laplace domain as suggested by Narayanan (1979).

$$L_k = \frac{\sin\left(\frac{k\pi}{N}\right)}{\left(\frac{k\pi}{N}\right)} \tag{A.2}$$

when $k = 0$, $L_0 = 1$.

## References


Adey, R.A., Brebbia, C.A., 1973. Efficient method for solution of viscoelastic problem. Journal of Engineering Mechanics Division—ASCE 99, 1119–1127.

Aköz, A.Y., Kadıoğlu, F., 1996. The mixed finite element solutions of circular beam on elastic foundation. Computers and Structures 60 (4), 643–657.

Aköz, A.Y., Kadıoğlu, F., 1999. The mixed finite element method for the quasi-static and dynamic analysis of viscoelastic Timoshenko beams. International Journal for Numerical Methods in Engineering 44, 1909–1932.

Chapra, S.C., Canale, R.P., 1998. Numerical Methods for Engineers, third ed. McGraw-Hill.

Chen, T., 1995. The hybrid Laplace transform/finite element method applied to the quasi-static and dynamic analysis of viscoelastic Timoshenko beams. International Journal for Numerical Methods in Engineering 38, 509–522.

Chen, W.H., Lin, T.C., 1982. Dynamic analysis of viscoelastic structure using incremental finite element method. Computers and Structures 4, 271–276.

Christensen, R.M., 1982. Theory of Viscoelasticity, second ed. Academic Press, New York.

Durbin, F., 1974. Numerical inversion of Laplace transforms: an efficient improvement to Dubner and Abate's method. The Computer Journal 17, 371–376.

Eringen, A.C., 1982. Mechanics of Continua. John Wiley and Sons, New York.

Findley, W.N., Lai, J.S., Onaran, K., 1976. Creep and Relaxation of Nonlinear Viscoelastic Material. North-Holland, New York.

Flügge, W., 1975. Viscoelasticity, second ed. Springer, Berlin.

Ilyasov, M.H., Aköz, A.Y., 2000. The vibration and dynamic stability of viscoelastic plates. International Journal of Engineering Sciences 38, 695–714.

Kadıoğlu, F., Aköz, A.Y., 1999. The mixed finite element method for the dynamic analysis of viscoelastic circular beams. In: Fourth International Conference on Vibration Problems, Calcutta, India, November 27–30, pp. 40–52.

Kim, T.W., Kim, J.H., 2001. Parametric instability of a cross-ply laminated beam with viscoelastic properties under a periodic force. Composite Structuress 51, 205–209.

Kıral, E., Ertepınar, A., 1974. Studies on elastic rods subject to diverse external agencies. Part III: vibrational analysis of space rods. METU Journal of Pure and Applied Science, 55–69.

Kıral, E., Tokdemir, T., Ural, S., 1976. Transient response of an elastic or/and viscoelastic curved rod under arbitrary time dependent loading. METU Journal of Pure and Applied Sciences 9, 63–86.

Narayanan, G.V., 1979. Numerical Operational Methods in Structural Dynamics. Ph.D. thesis, University of Minnesota, Minneapolis, MN.

Park, S.W., 2001. Analytical modeling of viscoelastic dampers for structural and vibration control. International Journal of Solids and Structures 38, 8065–8092.

Park, S.W., Schapery, R.A., 1999. Methods of interconversion between linear viscoelastic material function. Part I—a numerical method based on Prony series. International Journal of Solids and Structures 36, 1653–1675.

Schapery, R.A., Park, S.W., 1999. Methods of interconversion between linear viscoelastic material function. Part II—an approximate analytical method. International Journal of Solids and Structures 36, 1677–1699.

Sokolnikoff, I.S., Redheffer, R.M., 1958. Mathematics of Physics and Modern Engineering. McGraw-Hill, Tokyo.

Spiegel, M.R., 1965. Theory and Problems of Laplace Transforms. In: Schaum's Outline Series. McGraw-Hill.

Temel, B., Çalım, F.F., 2003. Forced vibration of cylindrical helical rods subjected to impulsive loads. Journal of Applied Mechanics—ASME 70 (2), 281–291.

White, J.L., 1986. Finite element in linear viscoelasticity. In: Proceeding 2nd Conf. on Matrix Method in Structural Mechanics AFFDL-TR-68-150, pp. 489–516.

Yamada, Y., Takabatake, H., Sato, T., 1974. Effect of time dependent material properties or dynamic response. International Journal for Num. Methods Engineering 8, 403–414.

Yerli, H.R., Temel, B., Kıral, E., 1998. Transient infinite elements for 2D soil-structure interaction analysis. Journal of Geotecnical and Geoenviromental Engineering 124 (10), 976–988.